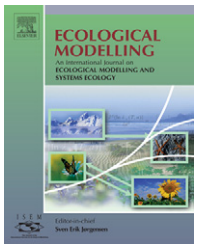
available at www.sciencedirect.com

ScienceDirect

journal homepage: www.elsevier.com/locate/ecolmodel



Dynamic compartment approach for modelling regimes of carbon cycle functioning in bog ecosystems

*Nikolay N. Zavalishin**

Laboratory of Mathematical Ecology, A.M. Obukhov Institute of Atmospheric Physics, Russian Academy of Sciences, 3 Pyzhevsky Lane, Moscow 119 017, Russian Federation

ARTICLE INFO

Article history:
Received 25 August 2007
Received in revised form
11 December 2007
Accepted 12 December 2007
Published on line 20 February 2008

In memoriam Yuri M. Svirezhev—the brilliant Scientist, perfect Teacher, outstanding Person.

Keywords:
Compartment dynamic model
Ecosystem "storage-flow" diagram
Bifurcation analysis
Carbon cycle

ABSTRACT

Svirezhev's method of dynamic model design by a given "storage-flow" diagram [Svirezhev Y.M., 1997. On some general properties of trophic networks. Ecol. Model. 99, 7–17] is developed and used for investigating dynamic regimes of carbon cycle functioning in a typical boreal transitional bog ecosystem. Ecosystems are often represented by static "storage-flow" diagrams reflecting their structure and matter or energy transfer between components at fixed time moments. Using the data of such diagrams aggregated in ecological field studies one can construct a dynamic model of the ecosystem to predict its future behaviour and to estimate a response to external perturbations—natural and human. Stability of both current equilibrium and possible alternative steady states and more complicated attractors are studied under two types of parameter perturbation: CO_2 atmospheric concentration increase initiated by greenhouse effect, and change in the rate of carbon output from dead organic matter and litter which depends on the water table level and possible peat excavation. Calculation of bifurcation curves gives areas in the parameter space where stable functioning of carbon cycle is provided. Steady states can be interpreted as raised bog, meadow, forest and fen. CO_2 concentration increase leads the current state of transitional bog to loose stability with appearance of oscillatory dynamics and further evolution to the chaotic attractor. The model is rich by chaotic solutions serving as transition regimes between regular steady and periodic attractors. Another chaotic regime is formed from forest equilibrium and exists in the same area of phase space where current equilibrium is stable.

© 2007 Elsevier B.V. All rights reserved.

1. Introduction

1.1. *Compartment dynamic approach in modelling ecosystem structure and functioning*

Since first works of Patten (1982), a compartment approach based on "storage-flow" diagrams aggregated in the field studies became popular for ecologists to analyze ecosystem structure and functioning. The diagram with storages of matter or energy in compartments and flows between them reflects both the state of ecosystem at the fixed time moment (a year is a typical time unit) and a complexity of its structure. Most of natural ecosystems can be represented as networks with complicated connections between components that interact to each other in a nonlinear way. Hence, there are two key features of ecosystems any researcher should pay attention to: complexity of structure and nonlinearity of functioning. Both of them initiate complex diagrams of "storage-flow" type but cannot be adequately analyzed by use of such schemes due to their static nature. Static methods of compartment analysis include environ approach (Gattie et al., 2006) which allows to estimate average time of residence of matter in the

* Tel.: +7 495 951 2170; fax: +7 495 953 1652.
E-mail address: nickolos@ifaran.ru.
0304-3800/$ – see front matter © 2007 Elsevier B.V. All rights reserved.
doi:10.1016/j.ecolmodel.2007.12.006

given compartment, the probability for a particle of matter to enter or to leave a particular block, indirect effects in the matter cycle functioning and different types of cycling indices (Patten, 1985,1992; Higashi and Patten, 1986; Borrett et al., 2006). Another methods are based on using some information measures like average mutual information and ascendency (Ulanowicz, 1986; Ulanowicz and Abarca-Arenas, 1997) which gives the representation of how effectively an ecosystem is organized in order to utilize available resources. Hypothesis of static econetwork as a Markov chain serves a foundation to all those modelling techniques. Attempts undertaken by some authors to expand ascendency on the dynamic case with continuous time failed due to fundamental problems with a correct definition of mutual information in that case. A partial success was only achieved for discrete time ecological networks (Higashi et al., 1993; Pahl-Wostl, 1995). The static formalism and network flow analysis algorithms are realized in some successful software packages: EcoPath (Christensen and Walters, 2004), NetMatCalc (Latham, 2006): Wand (Allessina and Bondavalli, 2004), NEA (Fath and Borrett, 2006), and EcoNet (Kazanci, 2007). Some new concepts have been also developed: network synergism (Fath and Patten, 1998), network virtual amplification and resource homogenization (Fath and Patten, 1999).

Dynamic behaviour of ecosystems expressed by "storage-flow" diagrams, and their reaction to anthropogenic stress or climatic changes can be represented only by use of a dynamic model. The problem how to construct a dynamic compartment model by a given "storage-flow" diagram is in turn complicated and mathematically incorrect since infinitely many systems can be designed on the same data set. It means that we need some additional hypotheses to make a definite choice among the set of all dynamic systems possible for a particular compartment scheme. One type of hypotheses initiated by biogeochemical investigations of Savageau (1970) was adopted to ecological problems by Voit and Sands (1996) and founded on using "power law" functions as full input and output fluxes for each ecosystem compartment. That set gave rise to use of a canonical S-systems method in compartment ecology. Another set of hypotheses was suggested by Svirezhev (1997) and Jorgensen and Svirezhev (2004) and has simple and clear physical explanation relatively to possible functional dependence of flows on storages as model variables. Novelty of his approach is provided both by its general applicability to any ecosystem represented by a compartment scheme, and some universality in selection of flow functions that allows to account for nonlinearity of interactions between compartments and simultaneously reflect expert knowledge on ecosystem structure and functioning. Further we give a short overview of his method following Svirezhev (1997) and describe some features of resulting dynamic system.

Let $x_i(t)$ be the storage of matter or chemical element in ith compartment, q_i the input flow from the environment to the compartment i, y_i the output flow from reservoir i to the environment and f_{ij} is the internal flow from ith block to jth (Fig. 1). All of them can be functions of storages and/or time and are called *flow functions*. The key assumptions of Svirezhev's method are (Svirezhev, 1997):

1. The given diagram is flow-balanced: $q^* + f^* = y^*$, i.e. the current scheme represents a steady state of the dynamic system.
2. Intercompartment flows are determined by storages of only two participating compartments: $f_{ki} = f_{ki}(x_k, x_i)$ and $f_{ik} = f_{ik}(x_i, x_k)$.
3. Each input flow does not depend on the corresponding storage and can be thought of either as a constant or as time-dependent function: $q_i = \text{const.}$ or $q_i = q_i(t)$.

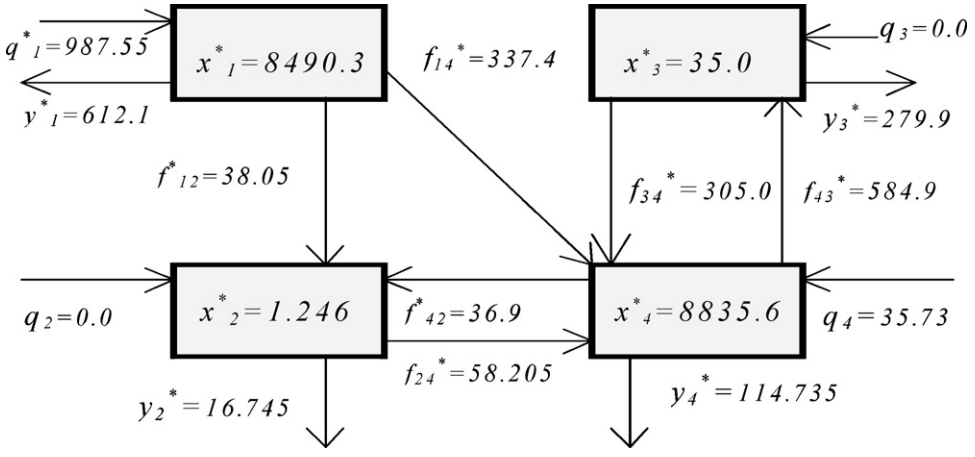


Fig. 1 – Aggregated "storage-flow" diagram of the carbon cycle structure and functioning in the mesotrophic bog ecosystem (Alexandrov et al., 1994). Storages (in g/m^2 of dry matter): x_1, plants; x_2, animals; x_3, fungi and bacteria; x_4, dead roots, trees and litter. Input flows (in g/(m^2 year) of dry weight): q_1, assimilation by plants; q_4, input from surrounding ecosystems. Output flows (in g/(m^2 year) of dry weight): y_1, respiration of vegetation, consumption by phytophages from other ecosystems; y_2, animal respiration; y_3, fungal and bacterial respiration; y_4, runoff, peat formation and abiotic oxidation. Intercompartment flows: f_{12}, consumption by phytophages; f_{14}, plant death (litterfall); f_{24}, animal death; f_{42}, consumption of dead organic matter by saprophages; f_{34}, dead bodies and excretions of fungi and bacteria; f_{43}, consumption of dead organic matter by fungi and bacteria.

4. Each output flow depends linearly on corresponding storages: $y_i(x_i(t)) = y_i^0 + m_i x_i(t)$. Since y_i^0 can be included into the input flow of ith compartment, then $y_i(x_i) = m_i x_i$.
5. Each of intercompartment flows belongs to the only control type:
   (a) flow f_{ki} depends on the sending storage x_k linearly, i.e. $f_{ki} = \alpha_{ki} x_k$, *donor type*;
   (b) flow f_{ki} is determined only by the storage of receiving compartment and depends on it also in the linear way, i.e. $f_{ki} = \beta_{ki} x_i$, *recipient type*;
   (c) flow f_{ki} depends only on the product of storages in both participating compartments, that corresponds to the classical ecological relationship of the *Lotka–Volterra type*: $f_{ki} = \gamma_{ki} x_i x_k$.

Donor and recipient linear types of flow control are traditionally used in the compartment ecological modelling whereas the Lotka–Volterra flow function represents the simplest possible nonlinear type of interaction between two particular blocks. The assumption 5 allows one to calculate all undetermined coefficients by the only given "storage-flow" diagram:

$$\alpha_{ki} = \frac{f_{ki}^*}{x_k^*}, \qquad \beta_{ki} = \frac{f_{ki}^*}{x_i^*}, \qquad \gamma_{ki} = \frac{f_{ki}^*}{x_k^* x_i^*}, \qquad m_i = \frac{y_i^*}{x_i^*} \tag{1.1}$$

This assumption not only gives some feasibility for the researcher to describe intercompartment flow dependences usually having an uncertain form, but also set a serious limitation that cannot be overcome in the framework of only one flow-balanced diagram. If the diagram is not flow-balanced we can consider it as a current state of the ecosystem for the given time moment and make a dynamic model without assumption 1.

Following assumptions 1–5 and using the data from the measured "storage-flow" scheme, we can construct the system of ordinary differential equations for the ecosystem under study:

$$\frac{dx_i}{dt} = q_i + \sum_{s=1}^{n} b_s^i x_s + x_i \sum_{s=1}^{n} c_{is} x_s, \quad i, s = 1 \dots n, \tag{1.2}$$

where matrices B and C are expressed through coefficients of flow functions by the formulas:

$$b_i^s = \begin{cases} -m_i + \sum_{k \neq i} (\beta_{ki} - \alpha_{ik}), & i = s; \\ \alpha_{si} - \beta_{is}, & i \neq s. \end{cases}, \quad c_{is} = \gamma_{si} - \gamma_{is}. \tag{1.3}$$

The system (1.2) is called *Svirezhev's dynamic compartment model*. Consequently, the selection of flow function types for intercompartment exchange determines "the level of nonlinearity" of the obtained dynamic model. Although the general problem of maximally appropriate for the given ecosystem flow control selection has not been solved yet, we can use one, natural in some sense, criterion: the selection is considered to be adequate if equilibrium of the dynamic system, given by the diagram, is locally stable, since only stable states of ecosystems can really be observed in nature (Zavalishin and Logofet, 2001).

Note that Eq. (1.2) can be interpreted in two different ways. On the one hand, they can be thought of as a nonlinear extension of an analytically solvable linear differential system, and on the other—as a linear extension of the Lotka–Volterra model traditional for mathematical ecology, where in the equation for each variable linear terms on other variables are added. Thus, besides the problems of ecological modelling, systems of Svirezhev's class have a pure mathematical interest. In particular, conditions for invariance of the non-negative cone in the phase space and a theorem on dissipativity were proved in (Zavalishin and Logofet, 1997). Another practically important issue appears if all intercompartment flows are of Lotka–Volterra type: in this case Jacobi matrix of the current equilibrium, easily calculable directly from the flow-balanced diagram, is called a Svicobian and initiates a new concept of matrix stability—DaD-stability, which is independent of quantitative estimates of compartment storages and flows (Logofet, 1997).

In the present paper we apply Svirezhev's approach to the "storage-flow" diagram of the carbon cycle in the Tajozhny Log transitional bog ecosystem. The main objective of the work is to make conclusions about stability of its current equilibrium, existence of alternative biologically interpretable steady states and their bifurcations under two types of external perturbations: change of the rate of carbon output from dead organic matter and litter due to the human activities, and increase of the CO_2 assimilation by surface vegetation from the atmosphere initiated by the climate change. This goal concerns the problem of ability for bog ecosystems to compensate the carbon pressure by means of storaging carbon abundances from atmosphere (fertilization effect). We show that Svirezhev's dynamic approach together with methods of bifurcation theory can really help in solving such problems because they allow one to obtain additional results in modelling successions of bog ecosystems.

This paper is organized as follows. Section 2 describes the carbon cycle of Tajozhny Log mesotrophic bog ecosystem and results of its previous studies by static and dynamic compartment methods. Then we select flow control types for a dynamic compartment model based on Svirezhev's algorithm. Further, in Section 3 stability and local bifurcations of a raised bog and a fen ecosystem are investigated as well as those for a meadow and a forest alternative equilibrium states in Section 4. Special attention is paid to the feasibility conditions of these states. All equilibria for the dynamic model are obtained analytically and interpreted from ecological point of view, the partial (local) bifurcation portrait of the model is formed. Section 5 is devoted to the problem of the ecosystem reaction to the atmospheric CO_2 concentration increase resulting in an increasing of carbon assimilation by plants. Another important parameter in this investigation is the rate of carbon output from dead organic matter and litter due to the human activities, like peat mining, or natural disturbances, like fires, that can corrupt the bog surface layer. Section 6 shows the complex structure of transient regimes between different equilibria and describes periodic solutions and chaotic attractor appearing with further increase of external carbon pressure.

2. Storage-flow diagram for the carbon cycle in Tajozhny Log mesotrophic bog and the compartment dynamic model

Fig. 1 illustrates the static compartment model of carbon cycling in a mesotrophic bog ecosystem that has been obtained by use of aggregating the data from field studies carried out during 20 years at the experimental area Tajozhny Log (Novgorod Region) of the Institute of Geography, Russian Academy of Science (Bazilevich and Tishkov, 1986; Alexandrov et al., 1994). There are some reasons to select a transitional bog ecosystem as an object to be modelled and simulated by mathematical methods. The first is an importance of bogs in the planetary climate–biota system as accumulators of carbon and regulators of the global carbon cycle. The second is a wide propagation of such type of bogs over the territory of Russia and the fact that bogs present in almost all biomes from tundra to tropical rainforests allowing one to consider mechanisms of carbon cycle functioning in them to be similar. Thirdly, there are sufficiently accurate vertical and horizontal boundaries separating Tajozhny Log transitional bog from neighboring ecosystems that have fundamentally different functioning from the biological viewpoint (Alexandrov et al., 1994). Those boundaries allow one to accurately separate intrinsic and output fluxes as well as to design complete compartment diagrams of carbon, nitrogen and mineral elements cycling. Data for the cycles were obtained during a number of years by different scientific groups from institutes of Russian Academy of Sciences as well as Russian State Committee for Hydrometeorology and appear to be reliable source of information on all aspects of the ecosystem behaviour. Furthermore, mesotrophic bog is an ecosystem of transitional type between a forest and raised oligotrophic bog, both of which can be final states of the bog evolution. Thus, evidence appears for potentially rich dynamic behaviour and a reason for creating and investigating of dynamic compartment model.

Peatland models grouped into two basic categories – conceptual and simulation – are reviewed in Yu et al. (2001a). Conceptual group is based on the Clymo peat growth model (Climo, 1984, 1992) which treats the accumulating peat as a two-layer system depending on the water table depth, type of the decay rates and thermal conditions. In simulation models, vegetation dynamics and spatial structure of carbon storage are integrated with a description of peat formation processes. These models serve to estimate effects of climate change on bog structure and functioning (Yu et al., 2001b). There exists a set of simulation models with integrated soil, hydrology and vegetation dynamics solving the same problems (Yu et al., 2002; Marsili-Libelli and Checchi, 2005), and furthermore, studying spatial structure of a bog's surface (Nungesser, 2003). In our case, a minimal set of storage-flow data allows one to construct dynamic model with equilibrium strictly coinciding with the measured storage-flow scheme under the minimal set of hypotheses. Nevertheless, the model has up to four additional biologically interpretable steady states and boundaries of their stability in a parameter space provide a rich dynamic behaviour with periodic and chaotic attractors.

Aggregated compartment scheme of carbon cycle in a mesotrophic bog consists of four reservoirs symbolizing carbon storage in plants, animals, fungi and bacteria, dead organic matter together with litter (Fig. 1). Plants serve as main source of carbon for animals and dead organic matter that is a food resource for decomposers represented by saprophagues included in the pool of animals, fungi and bacteria. Flows between compartments denote main biological processes in the bog: photosynthesis by vegetation, respiration of organisms, decomposition of litterfall, input from surrounding ecosystems, output for peat formation, abiotic oxidation and runoff. More details can be found in Alexandrov et al. (1994). Regarding observability of the current equilibrium as a sign of its stability, one can obtain the following, probably not unique from a plenty of possibilities, combination of flow functions having clear biological interpretation (Zavalishin and Logofet, 2001). Flows f_{12}, f_{14} cannot be selected in the recipient form and one flow from each pair (f_{34}, f_{43}), (f_{24}, f_{42}) must have Lotka–Volterra functional type as in a resource–consumer interaction (since they represent feeding and mortality processes). Also assimilation of plant carbon by animals is natural to depend on carbon storages in both pools ($f_{12} = \gamma_{12}x_1x_2$), reflecting resource–consumer relations between them, while death rate for the plant biomass is constant and a litterfall flow has a donor control type ($f_{14} = \alpha_{14}x_1$). Analogically, flows f_{24}, f_{34} (consumption of dead organic matter by decomposers) can also be established as donor type while f_{42}, f_{43} (mortality of decomposers) should be set in a nonlinear form due to resource–consumer relationship between litterfall and its decomposers—saprophages, fungi and bacteria. It means that the flow of dead organic matter from compartments 2 and 3 (animals and fungi with bacteria) are entirely determined by its storage in them, whereas back transformations of carbon depends on both biomasses of interacting carbon pools, since one of compartments participating in the interaction serves as a resource for another.

Flow $q_1 = \text{const.}$ is assumed constant since the intensity of carbon assimilation from the atmosphere due to photosynthesis can be considered approximately permanent in the annual time scale for such spatially local ecosystem. In general, due to fertilization effect CO_2 assimilation by terrestrial vegetation is a function with saturation on the atmospheric carbon content, and this is the reason why our parameterization is not completely adequate. However, this rule can be neglected for our particular ecosystem because we can make q_1 a bifurcation parameter changing proportionally to the atmospheric carbon concentration.

This selection of flow control types gives the nonlinear dynamic model of carbon cycle functioning in a transitional bog ecosystem:

$$\begin{aligned}
\frac{dx_1}{dt} &= q_1 - m_1x_1 - \alpha_{14}x_1 - \gamma_{12}x_1x_2,\\
\frac{dx_2}{dt} &= -m_2x_2 - \alpha_{24}x_2 + (\gamma_{42}x_4 + \gamma_{12}x_1)x_2,\\
\frac{dx_3}{dt} &= -m_3x_3 - \alpha_{34}x_3 + \gamma_{43}x_4x_3,\\
\frac{dx_4}{dt} &= q_4 - m_4x_4 + \alpha_{14}x_1 + \alpha_{34}x_3 + \alpha_{24}x_2 - x_4(\gamma_{43}x_3 + \gamma_{42}x_2).
\end{aligned} \tag{2.1}$$

Table 1 – Numeric values in the dynamic system (2.1)

Magnitude	Value
m	[0.0721; 13.439; 7.9971; 0.013]
α (non-zero elements)	$\alpha_{14}=0.0397$; $\alpha_{24}=46.7135$; $\alpha_{34}=8.7143$
γ (non-zero elements)	$\gamma_{12}=0.003597$; $\gamma_{42}=0.003352$; $\gamma_{43}=0.001891$
B	$\begin{pmatrix} -0.111834 & 0 & 0 & 0 \\ 0 & -60.152488 & 0 & 0 \\ 0 & 0 & -16.7114 & 0 \\ 0.0397 & 46.71135 & 8.7143 & -0.012986 \end{pmatrix}$
C	$\begin{pmatrix} 0 & -0.003597 & 0 & 0 \\ 0.003597 & 0 & 0 & 0.003352 \\ 0 & 0 & 0 & 0.001891 \\ 0 & -0.003352 & -0.001891 & 0 \end{pmatrix}$

Numerical values for the system parameters to be used in experiments are obtained from the data of the static "storage-flow" diagram and shown in Table 1.

The important and intriguing goal of the system modelling is to investigate an influence of an atmospheric CO_2 assimilation increase on dynamics of the carbon cycle and stability of its possible steady states. In terms of model (2.1), it means to study its qualitative behaviour depending on parameters q_1 and m_4 by means of bifurcation theory methods. Input flux q_1 denotes quantity of carbon assimilated from the atmosphere by vegetation due to photosynthesis, while parameter m_4 symbolizes the joint per capita rate of carbon output from dead biomass and litter. This rate allows one to simulate destruction of the soil surface layer that can be significantly changed due to peat mining. Joint impact of these two parameters reflect possible both natural (due to the climate change) and anthropogenic (peat mining activities) perturbations able to crucially transform organic matter cycling in a transitional bog ecosystem.

3. Simplest alternative steady states: stability of a raised bog and a fen

There are four possible steady states for system Eq. (2.1). All of them can be obtained analytically from the system of nonlinear algebraic equations:

$$\begin{aligned} &q_1 - m_1x_1 - \alpha_{14}x_1 - \gamma_{12}x_1x_2 = 0, \qquad -m_2x_2 - \alpha_{24}x_2 \\ &+(\gamma_{42}x_4 + \gamma_{12}x_1)x_2 = 0, \qquad -(m_3+\alpha_{34})x_3 + \gamma_{43}x_4x_3 = 0, \\ &q_4 - m_4x_4 + \alpha_{14}x_1 + \alpha_{24}x_2 + \alpha_{34}x_3 - x_4(\gamma_{43}x_3 + \gamma_{42}x_2) = 0, \end{aligned} \tag{3.1}$$

two of which have Lotka–Volterra type. It follows from the second equation that either

$$\text{(a)}\, x_2^* = 0, \quad \text{or} \quad \text{(b)}\, \gamma_{12}x_1^* + \gamma_{42}x_4^* = m_2 + \alpha_{24}, \tag{3.2}$$

and from the third one, that either

$$\text{(a)}\, x_3^* = 0, \quad \text{or} \quad \text{(b)}\, x_4^* = \frac{m_3+\alpha_{34}}{\gamma_{43}}. \tag{3.3}$$

Both $x_2^*=0$ and $x_3^*=0$ give $x_1^* = q_1/(m_1+\alpha_{14})$, then $x_4^* = (q_4/m_4) + (q_1\alpha_{14}/(m_1+\alpha_{14})m_4)$. This steady state corresponds to complete disappearing both animals and destructors except of plant communities and litter. Under given parameter values (see Table 1) $x^{(1)} = [8830.5; 0; 0; 2979.1]$ (g C/m^2) means that the ecosystem becomes a fen due to conservation of nondecomposed plant residues and can be formed as a result of natural (fires) or anthropogenic (drainage, peat excavation, etc.) transformations.

General dependence of the Jacobi matrix on dynamic system coefficients for the equilibrium $x^{(i)}$ has the form:

$$J^{(i)} = \begin{bmatrix} -m_1 - \alpha_{14} - \gamma_{12}x_2^{(i)} & -\gamma_{12}x_1^{(i)} & 0 & 0 \\ \gamma_{12}x_2^{(i)} & -m_2 - \alpha_{24} + \gamma_{42}x_4^{(i)} + +\gamma_{12}x_1^{(i)} & 0 & \gamma_{42}x_2^{(i)} \\ 0 & 0 & -m_3 - \alpha_{34} + +\gamma_{43}x_4^{(i)} & \gamma_{43}x_3^{(i)} \\ \alpha_{14} & \alpha_{24} - \gamma_{42}x_4^{(i)} & \alpha_{24} - \gamma_{43}x_4^{(i)} & -m_4 - (\gamma_{42}x_2^{(i)} + \gamma_{43}x_3^{(i)}) \end{bmatrix} \tag{3.4}$$

In the matrix $J^{(i)}$ elements $J_{22}^{(i)}$ and $J_{33}^{(i)}$ equal 0 due to Eq. (3.1) for those steady state points that have second and/or third corresponding coordinate to be 0.

Proposition 1. *Bifurcation curves for the equilibrium 1 are of transcritical type and have the form:*

$$\mathrm{TC}_{1,1}: \quad m_4 = \frac{\gamma_{43}}{m_3+\alpha_{34}}\left(\frac{q_1\alpha_{14}}{m_1+\alpha_{14}} + q_4\right), \tag{3.5}$$

$$\mathrm{TC}_{1,2}: \quad m_4 = \frac{\gamma_{42}(\alpha_{14}q_1 + q_4(m_1+\alpha_{14}))}{(m_1+\alpha_{14})(m_2+\alpha_{24}) - \gamma_{12}q_1} \tag{3.6}$$

Proof contained in Appendix A.

Direct calculation using Fig. 1 and Table 1 gives the straight line $\mathrm{TC}_{1,1}$: $m_4 \cong 4.02\times10^{-5}q_1 + 0.004$, and the curve $\mathrm{TC}_{1,2}$: $m_4 \cong (1.332\times10^{-4}q_1 + 0.0135)/(6.727 - 0.003597q_1)$. The intersection point M for these curves corresponds to the value

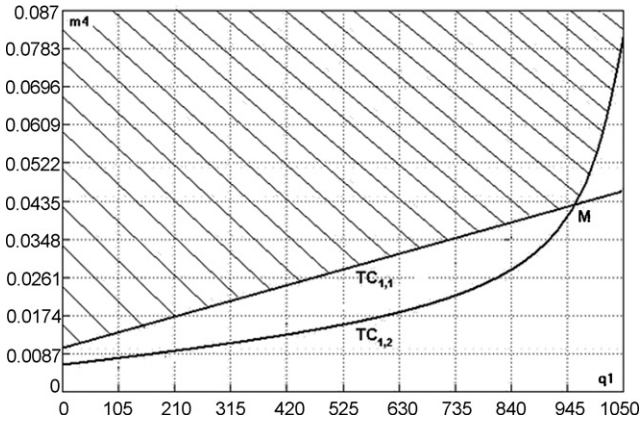


Fig. 2 – Bifurcation curves and basin of attraction for the equilibrium 1 (a fen). Bifurcation curves: $TC_{1,1}$, transcritical, merging with 2; $TC_{1,2}$, transcritical, merging with 3.

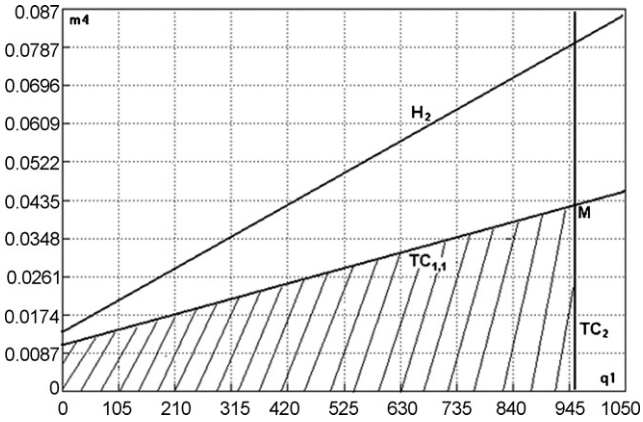


Fig. 3 – Stability domain and bifurcation curves for the equilibrium 2 (raised bog). Bifurcation curves: TC_2, merging with 4, $TC_{1,1}$, merging with 1, H_2, Hopf.

of input flow $q_1^* = K_1(m_1+\alpha_{14})/\gamma_{12}\gamma_{43} = 949.5\,\mathrm{g\,C/(m^2\,year)}$ where $K_1 = \gamma_{43}(m_2+\alpha_{24}) - \gamma_{42}(m_3+\alpha_{34}) = 0.05776$. The corresponding value for $m_4^* = 0.0422529$. At the point M two eigenvalues of the Jacobi matrix become zero resulting in Bogdanov–Takens bifurcation of codimension 2 (Kuznetsov, 2004). The second intersection point $(q_1^*; m_4^*) = (-(q_4(m_1+\alpha_{14})/\alpha_{14}); 0) = (-101.1; 0)$ belongs to the nonpositive orthant. Fig. 2 where computed curves and stability domain for the first equilibrium are depicted, shows that it is asymptotically stable either if the assimilation of the atmospheric CO_2 by plants is small compared to the modern value, or under high efflux velocities of carbon output from the system.

Conditions $x_2^* = 0$ and $x_4^* = (m_3+\alpha_{34})/\gamma_{43}$ from (3.3) immediately give $x_1^* = q_1/(m_1+\alpha_{14})$ from the first Eq. (3.1), as soon as $x_3^* = (1/m_3)(q_4 - m_4((m_3+\alpha_{34})/\gamma_{43}) + (\alpha_{14}q_1/(m_1+\alpha_{14})))$ follows from the fourth. This equilibrium numerically equal $x^* = [8830.5; 0; 34; 8835.6]\,(\mathrm{g\,C/m^2})$ lies on the hyperplain $x_2 = 0$ and implies absence of the animal compartment. It is easy to notice that amounts of carbon in plant and litter compartments do not differ from corresponding values at the current steady state. Biological sense of this steady state implies the raised bog which can usually be characterized by more poor plant species richness and low values of animal populations compared to the bog of a mesotrophic type (Tishkov, 1986).

Proposition 2. *Steady state 2 has three bifurcation curves:*

$$\textit{transcritical}\ TC_2: \quad q_1 = \left(m_2+\alpha_{24} - \gamma_{42}\frac{m_3+\alpha_{34}}{\gamma_{43}}\right)\frac{m_1+\alpha_{14}}{\gamma_{12}} = \textit{const.}; \tag{3.7}$$

$$\textit{transcritical}\ m_3\gamma_{43}x_3^{(2)} = 0\ \textit{which combines with}\ TC_{1,1};$$

$$\textit{Andronov–Hopf}\ H_2: \quad m_4 = \left(\frac{\alpha_{14}}{m_1+\alpha_{14}}q_1 + q_4\right)\frac{\gamma_{43}}{\alpha_{34}}. \tag{3.8}$$

Proof can be found in Appendix B.

Line TC_2 intersect two another lines $TC_{1,1}$ and $TC_{1,2}$ at the same point M: $m_4^* = (\gamma_{43}/(m_3+\alpha_{34}))((\alpha_{14}K_1/\gamma_{12}\gamma_{43}) + q_4) = 0.0422529$, and this fact makes a foundation to believe point M to be one of *organizing centers* of the whole bifurcation diagram (Kuznetsov, 2004), i.e. one of points with maximal codimension where bifurcation curves of less codimension have end-points. Direct computation gives $m_4 \cong 7.7125\times10^{-5}q_1 + 0.00778$ for the point M.

Regarding bifurcation curve H_2, one can notice that both equilibrium and periodic trajectory are unstable above the curve $TC_{1,1}$ and hence, curve H_2 does not generally affect stability properties of the second steady state. Fig. 3 with the parametric portrait shows that asymptotic stability of a raised bog takes place in the bounded domain in the parameter plane. This domain coincides with the domain of equilibrium positivity. Curve H_2 intersects $TC_{1,1}$ at the point $q_1^* = (q_4/\alpha_{14})(m_1+\alpha_{14}) = -101.1$ with the value $m_4^* = 0$. This point has a high codimension on the parametric portrait, since at most 3 bifurcation curves – $TC_{1,1}$, $TC_{1,2}$ and H_2 – intersect at it. Line TC_2 is intersected at another point

$$m_4^* = \frac{\gamma_{43}}{\alpha_{34}}\left(\frac{\alpha_{14}}{\gamma_{12}}\left(m_2+\alpha_{24} - \gamma_{42}\frac{m_3+\alpha_{34}}{\gamma_{43}}\right) + q_4\right) = 0.081031/\mathrm{year}$$

which corresponds to the presence of one zero and two complex conjugated eigenvalues in the spectrum of the Jacobi matrix.

Ecological interpretation of computed steady states can vary and is not highly reliable because evolution of real bog ecosystems is determined not only by dynamics of the carbon cycle but also by its interaction with the nitrogen cycle through C/N coefficients for vegetation fractions (Logofet and Alexandrov, 1983–1984a,b). Also it depends on the dynamics of a water table depth (Yu et al., 2002), which is not considered in this model. Nevertheless, these storage equilibrium configurations can believed potential climax states of the ecosystem whose reachability depends on their stability properties, whereas the measured steady state is of a transitional type between a forest and a raised bog. Since no plant species or species groups are considered in the model, naming steady states as forest, raised bog and fen can seem speculative. Nevertheless, it is founded on relations between numerical values of compartment biomasses (in carbon units) and comparison of them to real values for the given mesotrophic bog and neighboring raised bog and forests.

4. Meadow and forest: positivity, stability and local bifurcations

$$J^{(3)} = \begin{bmatrix} -m_1-\alpha_{14}-\gamma_{12}x_2^{(3)} & -\gamma_{12}x_1^{(3)} & 0 & 0 \\ \gamma_{12}x_2^{(1)} & 0 & 0 & \gamma_{42}x_2^{(3)} \\ 0 & 0 & -m_3-\alpha_{34}+\gamma_{43}x_4^{(3)} & 0 \\ \alpha_{14} & \alpha_{24}-\gamma_{42}x_4^{(3)} & \alpha_{24}-\gamma_{43}x_4^{(3)} & -m_4-\gamma_{42}x_2^{(3)} \end{bmatrix} = \begin{bmatrix} p & r & 0 & 0 \\ s & d & 0 & e \\ 0 & 0 & f & 0 \\ g & h & k & m \end{bmatrix} \tag{4.3}$$

Formulas (3.2(a)–3.3(b)) give conditions $x_3^* = 0$ and $\gamma_{12}x_1^* + \gamma_{42}x_4^* = m_2 + \alpha_{24}$ which consequently lead to expressions for x_4^* and x_2^*:

$$x_4^* = \frac{m_2+\alpha_{24}-\gamma_{12}x_1^*}{\gamma_{42}},$$

$$x_2^* = \frac{q_1-(m_1+\alpha_{14})x_1^*}{\gamma_{12}x_1^*} = \frac{q_1}{\gamma_{12}x_1^*} - \frac{m_1+\alpha_{14}}{\gamma_{12}}.$$

Substitution of them into the system (3.1) leads to a quadratic equation:

$$\begin{aligned} &\gamma_{12}(m_4\gamma_{12}-m_1\gamma_{42})x_1^{*2} + (q_4+q_1)\gamma_{42}\gamma_{12}x_1^* - (m_2+\alpha_{24})m_4\gamma_{12}x_1^* \\ &-(m_2+\alpha_{24})\gamma_{42}q_1 + (m_2+\alpha_{24})\gamma_{42}(m_1+\alpha_{14})x_1^* + \gamma_{42}\gamma_{12}m_4x_1^{*2} \\ &-\gamma_{42}\gamma_{12}(m_1+\alpha_{14})x_1^{*2} + \gamma_{42}\alpha_{24}q_1 - \gamma_{42}\alpha_{24}(m_1+\alpha_{14})x_1^* \\ &+\alpha_{14}\gamma_{42}\gamma_{12}x_1^{*2} = 0 \end{aligned}$$

with coefficients denoted by a, b, c:

$$\begin{aligned} a &= \gamma_{12}(m_4\gamma_{12}-\gamma_{42}m_1), \\ b &= \gamma_{42}\gamma_{12}(q_1+q_4) + \gamma_{42}m_2(m_1+\alpha_{14}) - m_4\gamma_{12}(m_2+\alpha_{24}), \\ c &= -(m_2+\alpha_{24})\gamma_{42}q_1 + \gamma_{42}\alpha_{24}q_1 = -m_2\gamma_{42}q_1 < 0, \end{aligned} \tag{4.1}$$

giving expressions for two possible equilibria:

$$\begin{aligned} x_1^* &= \frac{1}{2a}(-b \pm \sqrt{b^2-4ac}), \\ x_2^* &= -\frac{m_1+\alpha_{14}}{\gamma_{12}} + \frac{2aq_1}{\gamma_{12}(-b \pm \sqrt{b^2-4ac})}, \\ x_4^* &= \frac{m_2+\alpha_{24}}{\gamma_{42}} - \frac{\gamma_{12}}{2a\gamma_{42}}(-b \pm \sqrt{b^2-4ac}). \end{aligned} \tag{4.2}$$

Both of these theoretical equilibria correspond to disappearing of the destructors' compartment from the ecosystem. Under the given parameter values only $x_+^* = [3719.84; 42.72; 0; 13954.79]$ (g C/m^2) lies in the non-negative cone. Such a pair of steady states can potentially correspond in nature to a meadow (x_+^*) with sphagnum soil or a forested wetland like a sphagnum pinery (x_-^*) appearing as a result of a slow raising of the bog's bottom under the peat formation process (Razumovsky, 1981). This state is not a forest in the common sense due to the absence of the litter decomposition that usually is not accepted as a litter. However, such ecosystem can be an acceptor of the atmospheric CO_2 abundances. Stability and feasibility conditions together form domains of existence and attraction for both these steady states.

The Jacobi matrix for this pair of steady states has the form:

and is decomposable (reservoir 3 can be distinguished) thus permitting the cubic characteristic equation:

$$\lambda^3 + k_1\lambda^2 + k_2\lambda + k_3 = 0,$$

where coefficients are expressed through the matrix elements as $k_1 = -(p+m)$; $k_2 = -(eh+rs-pm)$; $k_3 = -reg + peh + mrs$. Routh–Hurwitz stability conditions are:

$$\begin{cases} -(p+m) > 0, \\ -(eh+rs-pm) > 0, \\ k_3 = mrs + peh - reg > 0, \\ R_3 = k_1k_2 - k_3 > 0 \end{cases} \tag{4.4}$$

First two inequalities (4.4) can be proved to fulfil iff $x_\pm^* > 0$ (see Appendix A). It means that stability boundaries are combined from the whole curves given by last two expressions (4.4) transformed into equalities and feasibility conditions which follow from (4.2):

$$\begin{cases} \dfrac{1}{2a}(-b \pm \sqrt{b^2-4ac}) \geq 0, \\ \dfrac{2aq_1}{-b \pm \sqrt{b^2-4ac}} \geq m_1+\alpha_{14}, \\ \dfrac{\gamma_{12}}{2a}(-b \pm \sqrt{b^2-4ac}) \leq m_2+\alpha_{24}. \end{cases} \tag{4.5}$$

Considering inequalities (4.5) under conditions $a>0$ and $a<0$ separately, one can derive that $x^{(3)} \in R_+^4$ iff its first component satisfies two inequalities:

$$\begin{cases} x_1^{(3)} \geq 0, \\ x_1^{(3)} \leq d = \min\left\{\dfrac{q_1}{m_1+\alpha_{14}}, \dfrac{m_2+\alpha_{24}}{\gamma_{12}}\right\}, \end{cases} \tag{4.6}$$

Corresponding boundaries of steady state feasibility are expressed through the system parameters using the substitution for the value d:either

$$m_4 = \frac{\gamma_{42}}{\gamma_{12}(m_2+\alpha_{24}-2(m_1+\alpha_{14}))}(\gamma_{12}(q_1+q_4)-(m_1+\alpha_{14})(m_2+2m_1)),$$

or

$$\begin{aligned} m_4 = \frac{\gamma_{42}}{2\gamma_{12}(m_2+\alpha_{24})^2}(&\gamma_{12}q_1(m_2-\alpha_{24}) - (m_2+\alpha_{24})(\gamma_{12}q_4 \\ &+(m_1+\alpha_{14})(m_2-2m_1))). \end{aligned}$$

By use of these expressions, inequalities (4.6) can be transformed into conditions for the plain of bifurcation parameters

$\{q_1, m_4\}$ limiting cones where each of steady states $x^{(3)} \in R^4_+$:

$$x^{(3)}_+ \notin R^4_+ \Leftrightarrow \begin{cases} m_4 < \dfrac{m_1\gamma_{42}}{\gamma_{12}} \\ m_4 > \dfrac{\gamma_{42}}{\gamma_{12}(m_2+\alpha_{24})}(\gamma_{12}(q_1+q_4)+m_2(m_1+\alpha_{14})) \end{cases} \tag{4.7}$$

and

$$x^{(3)}_- \notin R^4_+ \Leftrightarrow \begin{cases} m_4 > \dfrac{m_1\gamma_{42}}{\gamma_{12}} \\ m_4 < \dfrac{\gamma_{42}}{\gamma_{12}(m_2+\alpha_{24})}(\gamma_{12}(q_1+q_4)+m_2(m_1+\alpha_{14})) \end{cases}. \tag{4.8}$$

Bifurcation curves for the equilibrium 3 are described in the following.

Proposition 3. *There are three fold curves for the pair of forest-meadow equilibria*:

(a) $TC_{1,2}$, *corresponds to the merging of steady states* $x^{(1)}$ *u* $x^{(3)}$;
(b) $TC_{3,1}$, *is a saddle-node curve for the pair*:

$$m_4 = \frac{\gamma_{42}}{\gamma_{12}(m_2+\alpha_{24})^2}[-(\gamma_{12}(m_2-\alpha_{24})q_1 - \gamma_{12}q_4(m_2+\alpha_{24}) - m_2(m_1+\alpha_{14})(m_2+\alpha_{24})) \pm 2\sqrt{(q_1m_2\gamma_{12}[(m_2+\alpha_{24})(m_1\alpha_{24}-m_2\alpha_{14}) - \alpha_{24}\gamma_{12}(q_1+q_4)]}]; \tag{4.9}$$

(c) $TC_{3,2}$, *is a line in the plane* (q_1, m_4) *and has the following form*:

$$m_4(q_1) = \frac{\gamma_{43}(\alpha_{24}\gamma_{43}-\gamma_{42}(m_3+\alpha_{34}))}{K_1(m_3+\alpha_{34})}q_1 + \frac{\gamma_{43}q_4}{m_3+\alpha_{34}} + \frac{m_1\gamma_{42}(m_3+\alpha_{34}) - \gamma_{43}\alpha_{24}m_1 + m_2\alpha_{14}\gamma_{43}}{\gamma_{12}(m_3+\alpha_{34})}. \tag{4.10}$$

Proof is described briefly in Appendix C due to complicated algebraic transformations.

Complete feasibility and stability domains for meadow and forest steady states are depicted in Fig. 4. Curve $TC_{3,1}$ corresponds to the expression $b^2 - 4ac = 0$ (4.2) that denotes the condition of merging and disappearing of steady states $x^{(3)}_\pm$ (fold bifurcation). In Fig. 4 the third equilibrium absents in the inner part of the parabolic curve $TC_{3,1}$ with vertex at the point (978.57; 0.055448). Lines $TC_{3,2}$ and TC_2 intersect at the point

$$m_4^* = \frac{(m_2+\alpha_{24})\gamma_{43}\alpha_{14}}{\gamma_{12}(m_3+\alpha_{34})} + \frac{\gamma_{43}q_4}{(m_3+\alpha_{34})} - \frac{\gamma_{42}\alpha_{14}}{\gamma_{12}} = 0.042259,$$

coinciding with the point M, which therefore appears to be intersecting for the whole four bifurcation curves: $TC_{1,1}$, $TC_{1,2}$, TC_2 and $TC_{3,2}$. It follows that the second intersection point for the curves $TC_{3,2}$ и $TC_{1,2}$ except M can be found as a solution of the quadratic equation $p_0q_1^{*2} + p_1q_1^* + p_2 = 0$ with coefficients:

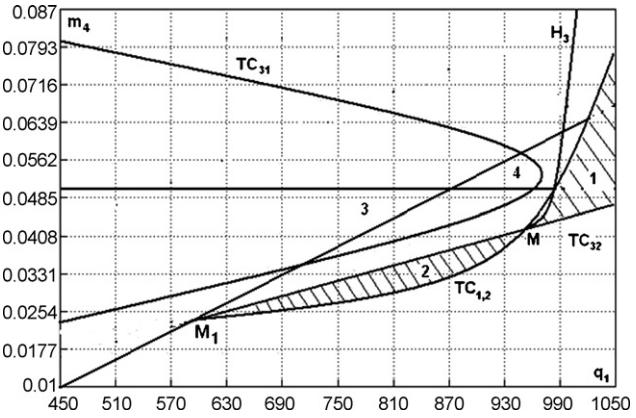


Fig. 4 – Bifurcation curves, domains of feasibility and stability for equilibria 3 (1-meadow, 2-forest). Bifurcation curves: $TC_{3,1}$, fold (merging of 3_+ and 3_-); $TC_{3,2}$, merging with 4; $TC_{1,2}$, merging with 1; H_3, Hopf bifurcation. Domains 3 and 4 illustrates formulas (4.7)–(4.8).

$$p_0 = \frac{\gamma_{12}\gamma_{43}}{K_1(m_3+\alpha_{34})}(\alpha_{24}\gamma_{43} - \gamma_{42}(m_3+\alpha_{34})) = 2.28\times10^{-7},$$

$$p_1 = \gamma_{42}\alpha_{14} - \frac{\gamma_{43}(\alpha_{24}\gamma_{43}-\gamma_{42}(m_3+\alpha_{34}))(m_1+\alpha_{14})(m_2+\alpha_{24})}{K_1(m_3+\alpha_{34})} + \frac{\gamma_{43}q_4}{m_3+\alpha_{34}} + \frac{m_1\gamma_{42}}{\gamma_{12}} + \frac{\gamma_{43}(m_2\alpha_{14}-m_1\alpha_{24})}{m_3+\alpha_{34}} = -3.58\times10^{-4},$$

$$p_2 = \gamma_{42}q_4(m_1+\alpha_{14}) - (m_1+\alpha_{14})(m_2+\alpha_{24}) \times \left(\frac{\gamma_{43}q_4}{m_3+\alpha_{34}} + \frac{m_1\gamma_{42}}{\gamma_{12}} + \frac{\gamma_{43}(m_2\alpha_{14}-m_1\alpha_{24})}{(m_3+\alpha_{34})\gamma_{12}}\right) = 0.134.$$

The solution is $q_1^* = 619.18\,\mathrm{g/(m^2\,year)}$ with $m_4^* = 0.0213199$. The point $M_1 = (q_1^*; m_4^*) = (619.18; 0.0213199)$ is a codimension 2 Bogdanov–Takens bifurcation point inducing curves depicted at Fig. 4. There is also Hopf bifurcation curve H_3 (corresponding to $R_3 = 0$) of complex implicit form limiting the stability domain of equilibria 3 which is hardly available by direct analytical investigation but can be calculated numerically by using the software package CONTENT (Kuznetsov, 1998).

5. Dynamics of the modern equilibrium under climatic and human-induced perturbations

Forecasting the reaction of terrestrial ecosystems to climate change in the long run is one of the most intrigueing challenges for ecological modellers. Any mesotrophic bog are known to change its biological state from a raised to a forest and vice versa (Bazilevich and Tishkov, 1986). Eigenvalues of the Jacobi matrix for the observed steady state are complex conjugate, and under current parameter values it is a focus. The Jacobi matrix is non-decomposible and has two zeros in the diagonal:

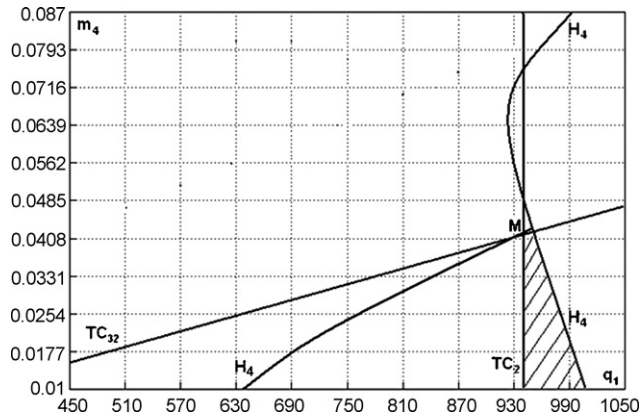


Fig. 5 – Parametric portrait for the equilibrium 4 (transitional bog): stability domains and critical curves. Bifurcation curves: TC_2, merging with 2; $TC_{3,2}$, merging with 3; H_4, Hopf.

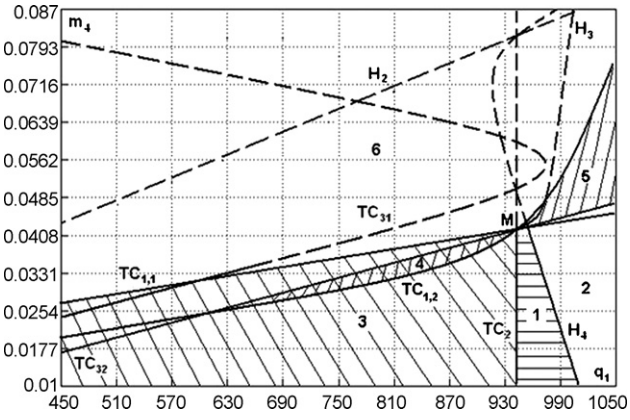


Fig. 6 – Local parametric portrait: stability domains for the model (3.1) steady states. Stability domains are denoted by digits: 1, stability domain for the current equilibrium; 2, oscillatory domain with periodic and chaotic solutions; 3, stability domain of a raised bog; 4, multistability domain: stable are a meadow and a raised bog; 5, forest wetland is stable (sphagnum pinery); 6, stability domain of a fen (all curves are denoted by a dotted line).

$$J^{(4)} = \begin{bmatrix} \frac{-q_1\gamma_{43}\gamma_{12}}{K_1} & -\frac{K_1}{\gamma_{43}} & 0 & 0 \\ \gamma_{12}x_2^{(4)} & 0 & 0 & \gamma_{42}x_2^{(4)} \\ 0 & 0 & 0 & \gamma_{43}x_3^{(4)} \\ \alpha_{14} & \alpha_{24} - \gamma_{42}\frac{m_3+\alpha_{34}}{\gamma_{43}} & -m_3 & -m_4 - \gamma_{43}x_3^{(4)} - \gamma_{42}x_2^{(4)} \end{bmatrix} = \begin{bmatrix} a & d & 0 & 0 \\ b & 0 & 0 & g \\ 0 & 0 & 0 & h \\ c & e & f & p \end{bmatrix} \quad (5.1)$$

From its characteristic equation that can be expressed in the form:

$$\lambda^4 - (a+p)\lambda^3 + \lambda^2[ap - (ge+fh+bd)] + \lambda[a(ge+fh) + d(bp-cg)] + bdfh = 0 \quad (5.2)$$

existence of two bifurcation curves in the parameter plane follows: (a) equilibrium transcritical curve $\Delta_4 = bdfh = 0$; (b) Andronov–Hopf bifurcation curve $\Delta_3 = 0$; under conditions $a_1 > 0$, $a_2 > 0$, $a_3 > 0$, where Δ_3 and Δ_4 are the 3rd and 4th Hurwitz determinants of the matrix $J^{(4)}$, a_1, a_2, a_3—coefficients of the characteristic polynomial (5.2). Transcritical curve $\Delta_4 = 0$ consists of two parts corresponding to the following expressions:

$$\frac{q_1\gamma_{43}}{\gamma_{43}(m_2+\alpha_{24}) - \gamma_{42}(m_3+\alpha_{34})} - \frac{m_1+\alpha_{14}}{\gamma_{12}} = 0,$$

$$q_1 + q_4 - \frac{m_1}{\gamma_{12}}\left(\alpha_{24} - \gamma_{42}\frac{m_3+\alpha_{34}}{\gamma_{43}}\right) - m_4\frac{m_3+\alpha_{34}}{\gamma_{43}} - m_2\left(\frac{q_1\gamma_{43}}{\gamma_{43}(m_2+\alpha_{24}) - \gamma_{42}(m_3+\alpha_{34})} - \frac{m_1+\alpha_{14}}{\gamma_{12}}\right) = 0,$$

First of them denotes transition into the equilibrium 2 at the line TC_2, while second is a transition to the equilibrium 3 since this part of the curve coincides with the line $TC_{3,2}$ (Fig. 5). Biological sense of these facts reflects possible paths of evolution for the measured state of the bog: either to the "nearest" raised bog, or into a meadow, or, in turn, into the sphagnum pine forest (Razumovsky, 1981). Stability domain for the given equilibrium 4 is also limited by the neutrality curve $\Delta_3 = 0$ that can be expressed in the form:

$$\Delta_3 = [a(ge+fh) + d(bp-cg)][-a(a+p) + d(ab+cg) + p(ge+fh)] - (a+p)^2bdfh = 0. \quad (5.3)$$

It can be interpreted as an implicit function dependence of m_4 on q_1 and should be resolved in the vicinity of the point M as an organizing center for the whole bifurcation diagram situated closed to the modern state of the ecosystem. Branches of the neutrality curve H_4, are obtained numerically by using the bifurcation software package CONTENT (Kuznetsov, 1998) and depicted in Fig. 5. Hence, to obtain the value of carbon input critical for the transitional bog state stability numerical methods are sufficient to use: under given $m_4 = 0.012986\, q_1^{cr} \approx 1010\,\mathrm{g\,C/(m^2\,year)}$ of the atmospheric carbon assimilation flow. This critical stability value of q_1 exceeds current value approximately in 8–10% and is essentially far from a hypothetical for many climate change scenarios double CO_2 concentration increase. The result can be considered as an evidence of the limited opportunity for bog ecosystems to accept carbon abundancies from the atmosphere without change of their qualitative state.

Although the observed steady state is stable in the domain 6 (see Fig. 6), it is situated near the right branch of the stability boundary H_4 and can intersect it as an assimilation of the atmospheric CO_2 by plants increases under the climate change. This intersection is accompanied by a supercritical Hopf bifurcation when the stable limit cycle $\Gamma_1^{(4)}$ appears under $q_1^{cr} \approx 1001.2\,\mathrm{g/(m^2\,year)}$. According to the standard theory (Kuznetsov, 2004), its period $T = 2\pi/|\lambda(q_1)| \approx 10.3$ years if $q_1 > q_1^{cr}$ with the amplitude $A \approx \sqrt{q_1 - q_1^{cr}}$ and equilibrium critical eigenvalues $\lambda_{1,2}(q_1^{cr}) = \pm 0.609\mathrm{i}$. Appear-

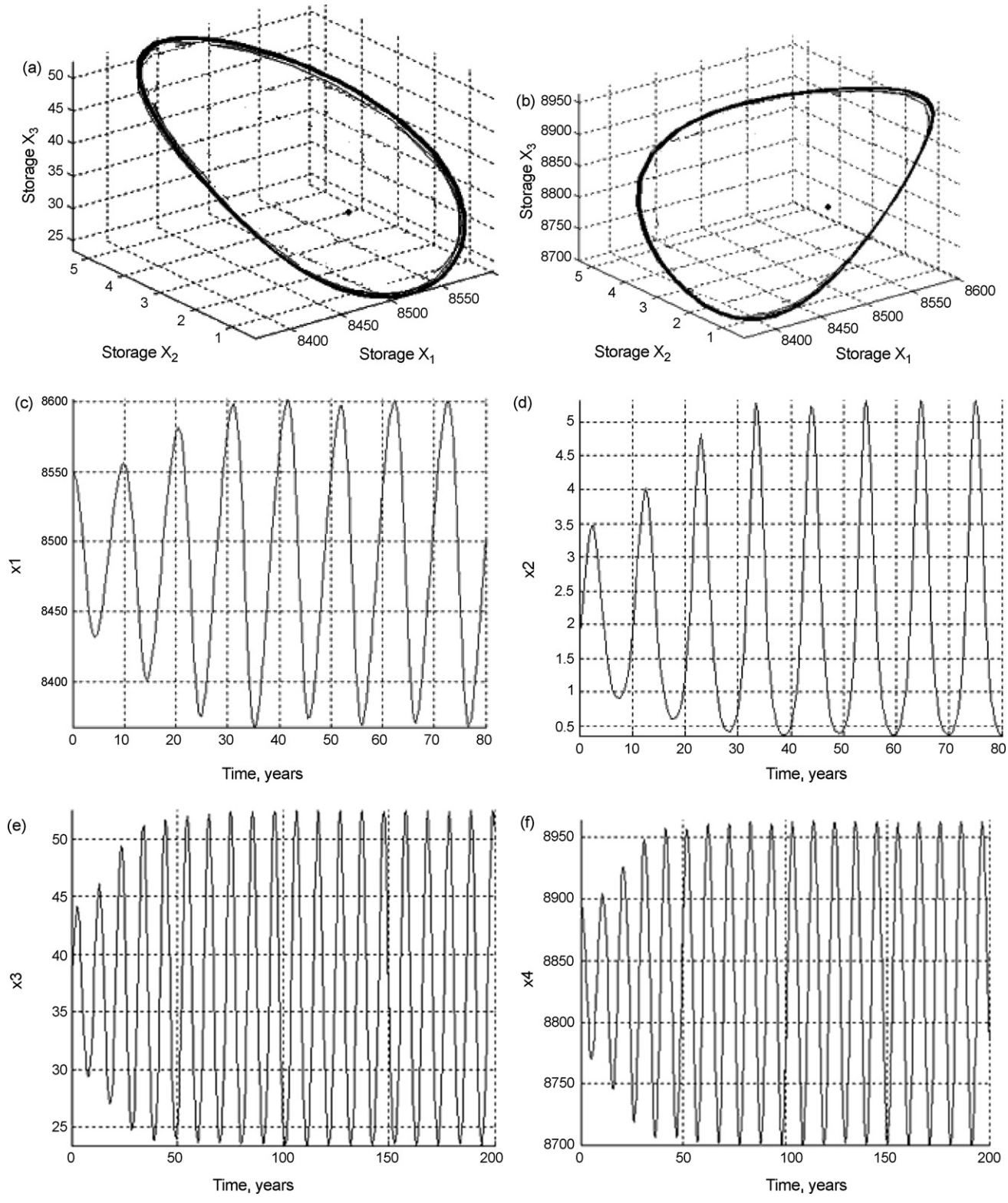


Fig. 7 – Limit cycle $\Gamma_1^{(4)}$ (two projections in a and b) as a result of Hopf bifurcation at the right part of the boundary H_4 for the transitional bog equilibrium. Time plots (c–f) are oscillatory and periodic for carbon in all compartments. Pairs (c–e) and (d–f) exhibits phase shift in oscillations of resource and consumer. $q_1 = 1010$ g/(m^2 year), $m_4 = 0.012986$. Initial conditions: $x_0 = [8550\ 1.8\ 36\ 8900]$ g/m^2.

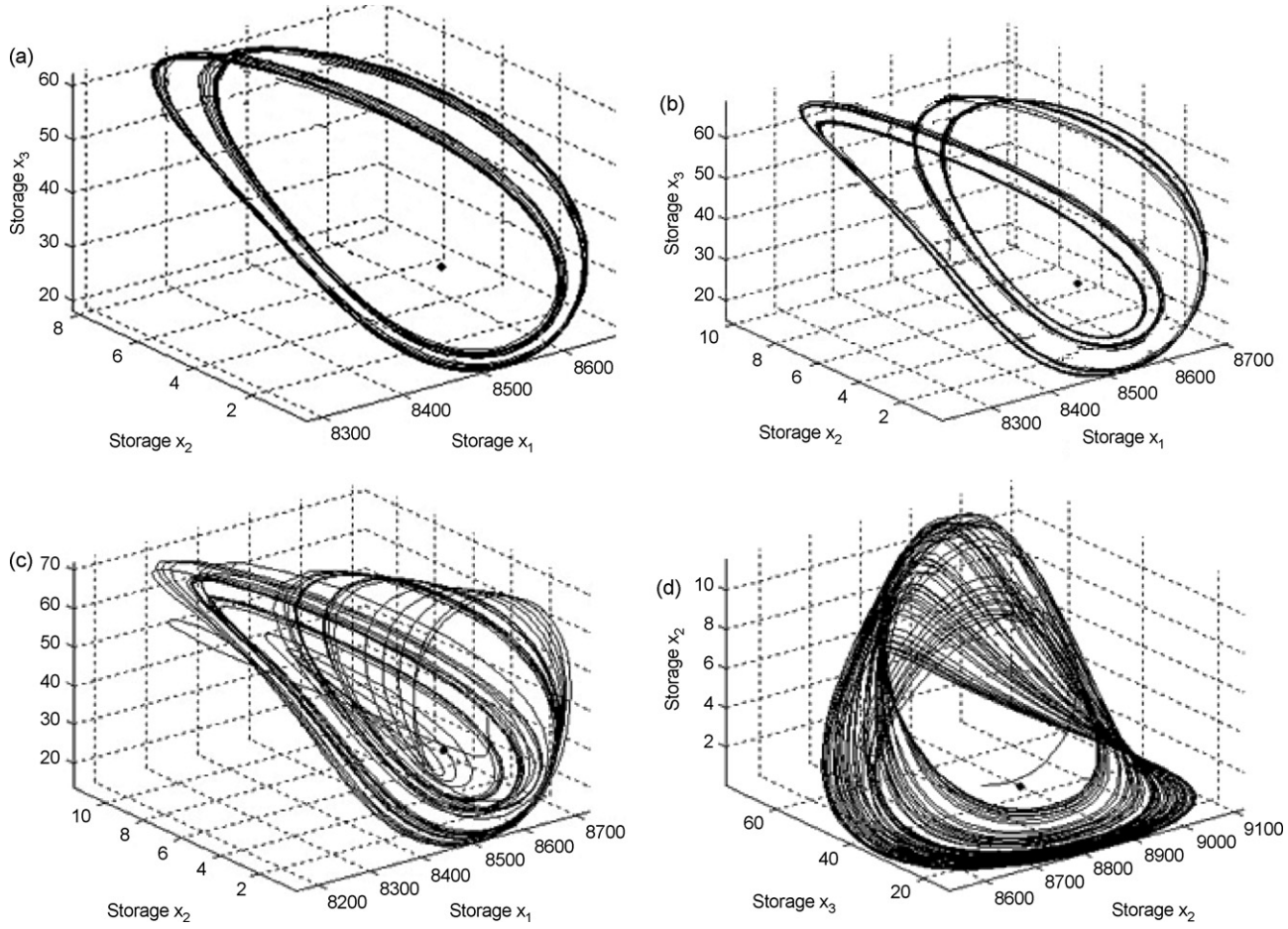


Fig. 8 – Limit cycles $\Gamma_2^{(4)}$ (a) and $\Gamma_4^{(4)}$ (b) as results of period-doubling bifurcation for the cycle $\Gamma_1^{(4)}$. $q_1 = 1018$ and 1025.25 g/(m^2 year). As $q_1 = 1027.6$ g/(m^2 year), strange attractor S_1 with irregular structure arises (c and d). $m_4 = 0.012986$. Initial conditions: $x^0 = [8550\ 1.8\ 36\ 8900]$ for cycles, $x^0 = [8600\ 2\ 34\ 8750]$ for the attractor. Lyapunov exponents for the attractor S_1: 1.25012, 0, −3.75438 and −3.86736.

ance of cyclic dynamics for carbon storages confirms that the opportunity of ecosystem to assimilate additional carbon from the atmosphere during climate change is restricted by the stability loss of the current state of the bog. Oscillatory regime appearing at the transition from the domain 1 into 2 looses its stability initiating a sequence of period-doubling bifurcations leading to the formation of a strange attractor at $q_1^q \approx 1027.6$ g C/(m^2 year) with strong instability of trajectories. Fig. 6 shows the limit cycle in the phase space and its temporal behaviours appearing under the Andronov–Hopf bifurcation. It can be seen from Fig. 7 that phase shift in oscillations look the same as those observed and modelled in population dynamics, considering vegetation and animals compartments as a resource–consumer system. This modelling result can be ecologically interpreted: as the available green phytomass diminishes, the biomass of the animals' compartment decreases since large animals stop attending the bog. Then, during next years, the green biomass is recovered and in some time animals come to this territory again feeding on young trees and shrubs. This biological mechanism of vegetation–animals interaction is called zoogenic succession and confirmed by observations at the experimental area Tajozhny Log (Tishkov, 1986).

Fig. 8 illustrates the period-doubling bifurcation resulting in a strange attractor formation. From ecological point of view, periodic and chaotic oscillations of carbon reservoirs correspond to obliteration of the transitional bog territory in turn by forestation and deforestation. The model shows that increasing of the carbon assimilation by plants due to the climate change leads to oscillations in the ecosystem carbon cycle functioning, fast in comparison with typical time scales of bog biochemical processes, and thus the stability of ecosystem steady state can be lost.

6. Periodic and chaotic regimes of carbon cycle functioning

Modern stationary configuration of carbon cycle can loose stability not only under increasing of carbon pressure but also as it is decreasing. The difference is only in the way the ecosystem adopts to changes of external perturbations: in the first case regular oscillatory dynamic regime starts from

the stable steady mesotrophic bog, while in the second the transitional bog is transformed into the raised one or into the meadow by a transcritical bifurcation. The state of raised bog is characterized by the absence of the animal compartment and is stable on the left of the line TC_2 and lower than the straight line $TC_{1,1}$ (domain 3 in Fig. 6). When increasing joint per capita rate of carbon output from dead biomass and litter, due to intensive peat formation or anthropogenic dranage, or fire, the transitional bog state is destabilized by the transcritical bifurcation at the straight line $TC_{1,1}$, and the system becomes a fen—an ecosystem with small carbon storage and absence of animals and destructors (and thus a good perspective for peat formation process). However, if $q_1 \in (619.2; 949.5)$, then another scenario can be realized. If the stability domain of the equilibrium 3 is large, the system appears in the domain 4 (Fig. 6) of the parameter space and converges to this state interpretable as a meadow growing by slow raising of the bog bottom initiated by strong peat formation process. Thus, the domain 4 is characterized by multi-stability when stable regime of carbon cycle functioning depends primarily on factors not allowed for in this model: the water table depth or nitrogen cycling. Fig. 9 exhibits a convergence of the system to equilibria 1 and 3 from close initial states.

Equilibrium 3 loses stability on the straight transcritical line $TC_{3,2}$, delivering it to the steady state 4 which belongs to the negative cone of the phase space under current parameter values. In domain 5 of the parametric portrait, under the high atmospheric carbon pressure and large values of litter decomposition intensity, another equilibrium $x_*^{(3)}$ from the pair 3 is stable. Due to the high carbon content in vegetation (almost twice higher than for the mesotrophic steady state), this equilibrium can be considered as a forest—sphagnum pinery which is formed the way as a meadow in the domain 4.

Numeric experiments show that multistability of attractors takes place also in the domain 1 where stability domain of the given equilibrium is relatively small in the phase space and an alternative chaotic attractor serves as a result of the evolution of the some limit cycle $\Gamma_1^{(3)}$. This cycle appears with small values of m_4 and exists in domains 1 and 3 at the parametric plain simultaneously with corresponding steady states. Evolution of the attractor under m_4 increase in the interval [0.008017. . .0.015713] is illustrated in Fig. 10. The first limit cycle (Fig. 10a and c) seems to appear as a result of a non-local bifurcation of the separatrix loop of the saddle and at $m_4 \approx 0.012431$ bifurcates into the cycle of double period (Fig. 11a and b). Time trajectories of the first cycle exhibits that frequency of oscillations for vegetation–animals subsystem is two-times less than that for litter-destructors subsystem (Fig. 10b and d). Period-doubling sequence starts at that point and leads to the strange sttractor S_2 (Fig. 11). The chaotic trajectory at Fig. 11 is interesting due to the remaining of a phase shift in oscillations of vegetation and animals—the resource–consumer subsystem of the carbon cycle. This feature is typical for the predator–prey interaction of species modelled in population biology but in this case it can be clearly seen in ecological network not consisting of biological species. For the chaotic attractor S_2 comparatively large maximal Lyapunov exponent (2.4504) confirms strong nonlinearity of the system in the parameter domain under study. As m_4 increases, this irregular set continues to exist in narrow domain of the phase space, and when $m_4 \approx 0.015713$, it suddenly disappears. The reason can lie in some non-local bifurcation but this problem is outside our research. Nevertheless, magnitude and the period of carbon content oscillations do not contradict to biological concepts on possible intervals of carbon storage changes in the bog ecosystem compartments.

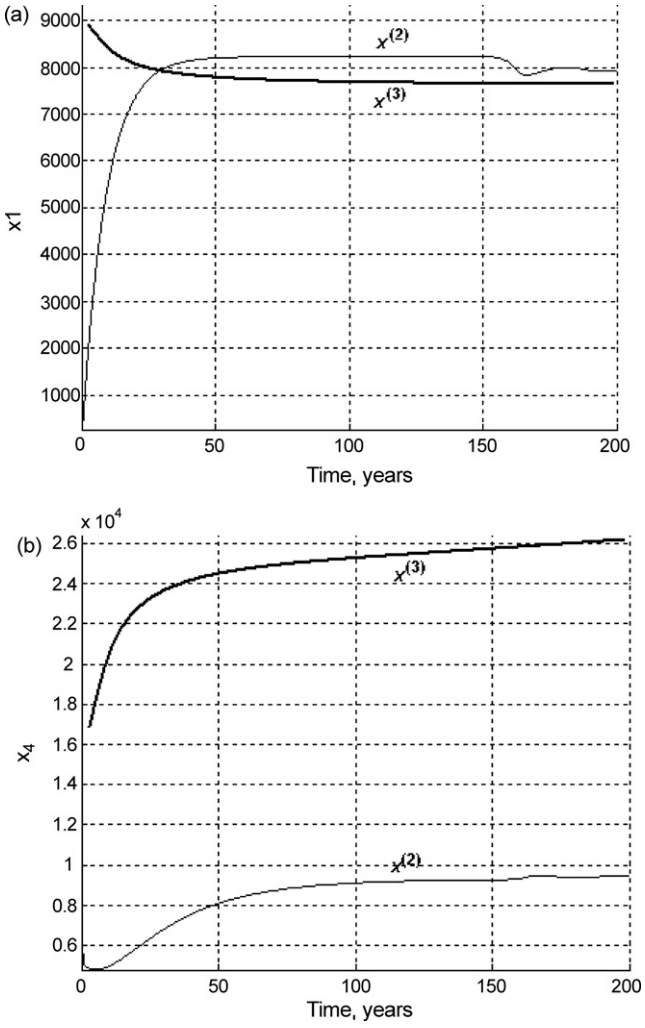


Fig. 9 – Multistability of equilibria in domain 4: convergence of time plots to steady states $x^{(2)}$ and $x^{(3)}$. Time trajectories of carbon storages in reservoirs 1 (a) and 4 (b). $q_1 = 920.55$ g/(m^2 year), $m_4 = 0.03913$. Equilibrium values: $x^{(2)} = [8231.4\ 0\ 2.16\ 8835.6]$ g/m^2; $x^{(3)} = [7945.2\ 1.12\ 0\ 26473]$ g/m^2.

7. Discussion and conclusions

Svirezhev's method gives one the opportunity to make dynamic compartment models and analyze regimes of their functioning leaning on the minimal set of data—one static storage-flow diagram, attracting expert knowledge on the

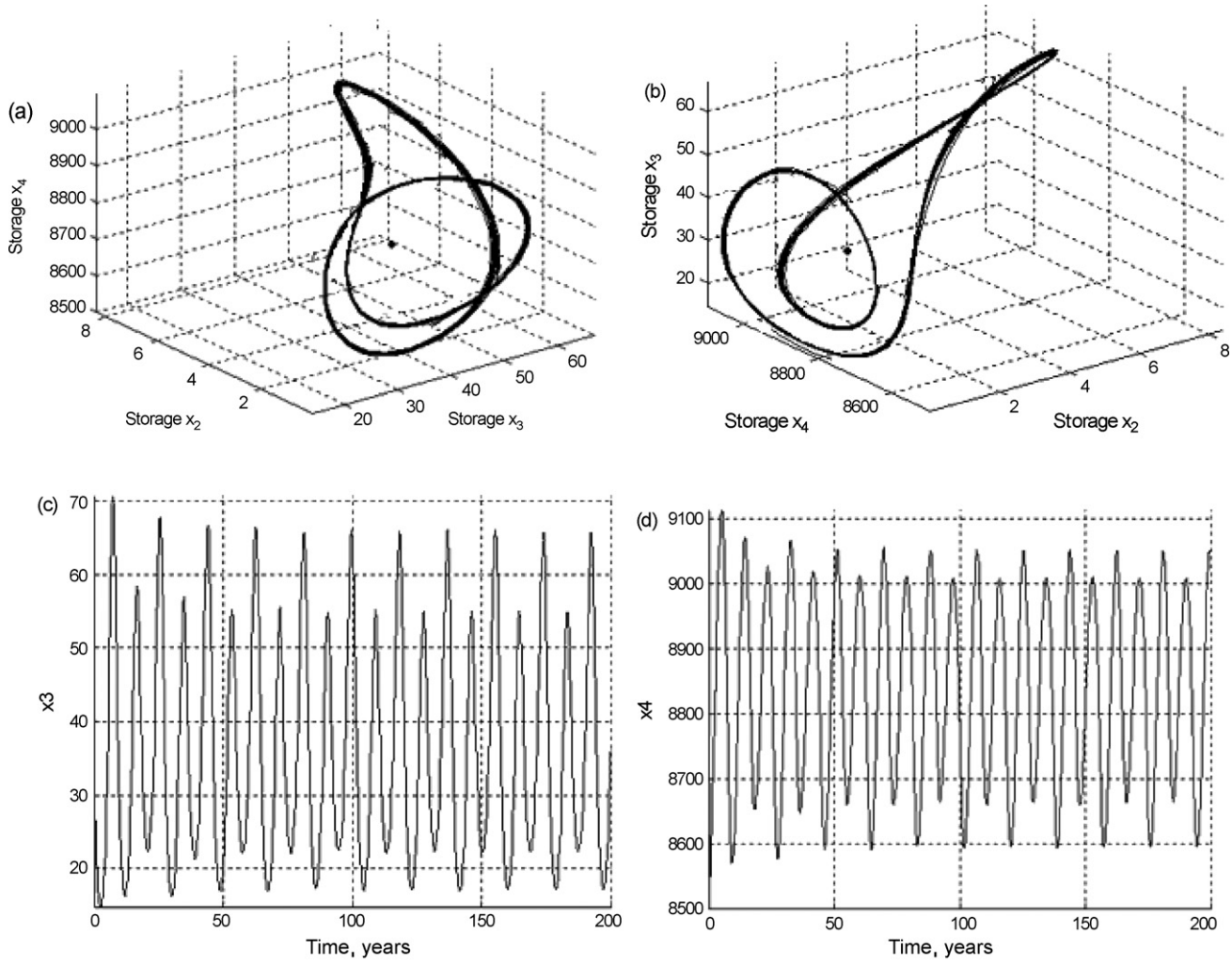


Fig. 10 – Projections of the limit cycle $\Gamma_1^{(3)}$ (a and c) and time plots for compartments x_3 and x_4 (b and d). $q_1 = 987.55$ g/(m^2 year), $m_4 = 0.01156$ and $x^0 = [8430\ 5.5\ 38\ 8500]$ g/m^2. Phase shift in oscillations of a resource–consumer subsystem is clearly observed.

control type for flow functions. Application of methods of bifurcation theory to Svirezhev's dynamic models allows one to estimate critical values of essential parameters including input flows depending on the environment–ecosystem interaction properties, and study stability boundaries in a parametric space. At the same time, the method stands out for its feasibility in selection of flow functions by expert biological or geographic knowledge. Note that classical dynamic approaches from mathematical ecology are still rare in research of large-scale "biogeographic" systems with matter or energy cycling, and this method represents one of successful attempts.

Applying Svirezhev's method to the particular mesotrophic bog ecosystem in the boreal zone of European Russia shows that along with biologically interpretable stationary states, the carbon cycle can exhibit complex oscillatory dynamic regimes, periodic and chaotic, which can be considered on the one hand as transitional between stationary ones under real parameter fluctuations, while on the other hand, have significantly large attractive domains in the phase space. In this context, the compartment dynamic model, even with only four pools, reflects complexity of functioning for interzonal mesotrophic bog ecosystems existing usually at the spatial boundaries of some zonal ecosystems. Elevation of the atmospheric CO_2 concentration yields an increase of carbon assimilation by bog's vegetation that results in a qualitative change of the carbon cycle dynamic behaviour—transfer firstly to periodic and then to chaotic oscillations of carbon content in compartments. This result confirms an evidence of the limited opportunity for bog ecosystems of a transitional (mesotrophic) type to accept carbon abundancies from the atmosphere without change of their qualitative behaviour. In contrast, decrease of the atmospheric carbon assimilation moves the ecosystem to the state of a raised bog, and if the output rate from the litter increases (due to either strengthening of peat formation or anthropogenic, or fire activities in litter destruction), then a meadow or a sphagnum pinery can arise. Intensification of dead biomass and litter decay transform the ecosystem in a state of a fen with neglectable amounts of carbon in animal and destructors pools. In all those cases

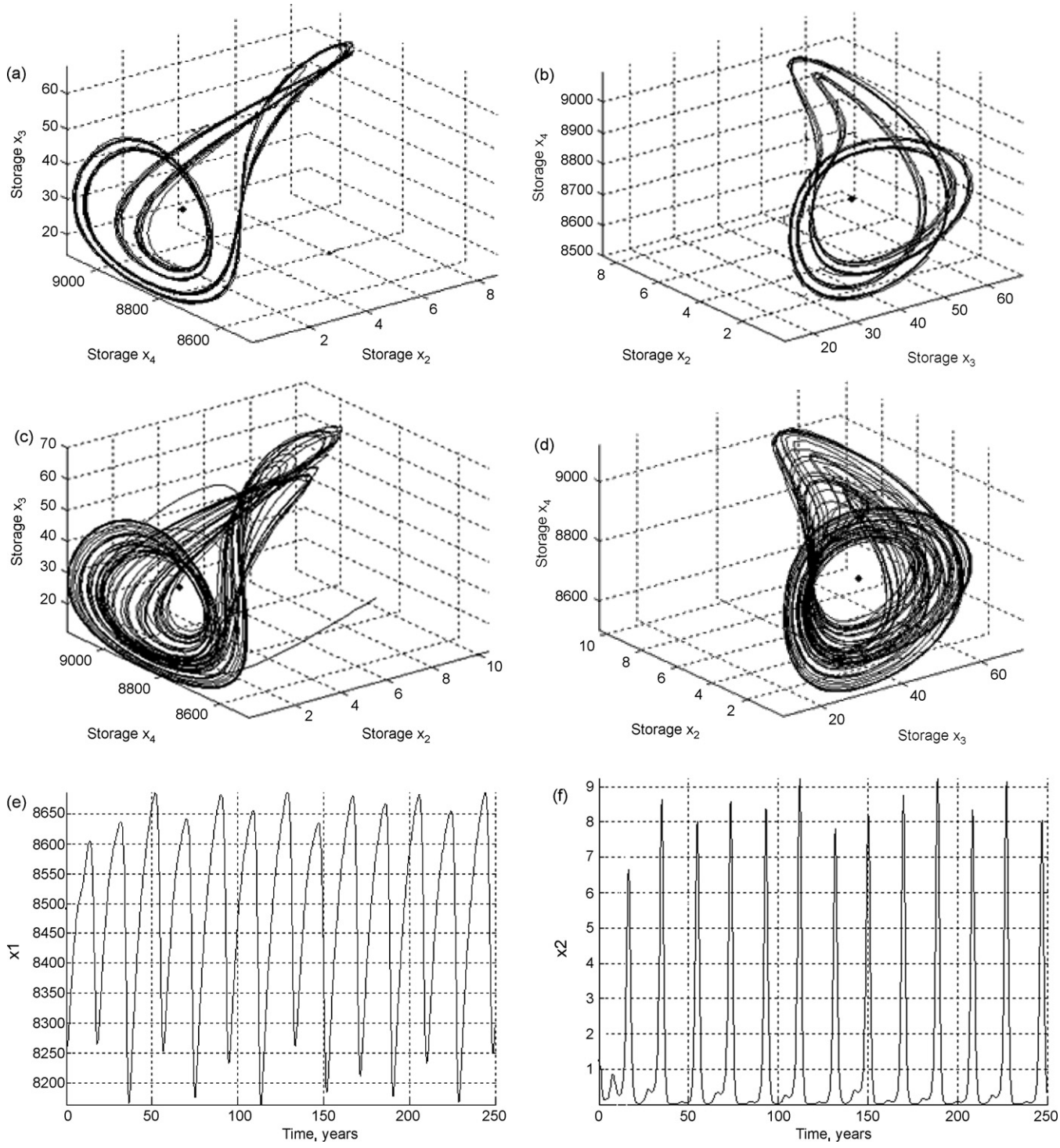


Fig. 11 – Limit cycle $\Gamma_2^{(3)}$ of a double period (a and b) and strange attractor S_2 (c and d). $m_4 = 0.012420$ (a and b) and $m_4 = 0.015249$ (c and d); $x^0 = [8300\ 7\ 38\ 8500]$ g/m^2.

both periodic cycles and chaotic attractors can serve not only as transient regimes but as particular limit set of the system. However, in such numeric experiments the dynamic system demonstrates a strong sensitivity to initial conditions that is not surprising for a nonlinear model, but unusual for such inertial ecosystem as a bog. It can be explained if we remind that dependence of carbon cycle parameters on another biophysical factors connected with nitrogen cycle and water regime are not taken into account. Hence, peculiarities of irregular attracting structures in the model phase space that are generated after stability loss of stationary states, can change as those factors are included in consideration. A lack of time series data from Tajozhny Log mesotrophic bog makes hardly available verifying of the model forecast

on the real ecosystem behaviour. In this case, it is important to make estimations of critical environment pressures on ecosystem from stability boundaries of its steady states. Svirezhev dynamic compartment approach significantly helps in this work.

$$J^{(2)} = \begin{bmatrix} -m_1-\alpha_{14} & -\gamma_{12}x_1^{(2)} & 0 & 0 \\ \gamma_{12}x_2^{(1)} & -m_2-\alpha_{24}+\gamma_{42}x_4^{(2)}+\gamma_{12}x_1^{(2)} & 0 & 0 \\ 0 & 0 & -m_3-\alpha_{34}+\gamma_{43}x_4^{(2)} & \gamma_{43}x_3^{(2)} \\ \alpha_{14} & \alpha_{24}-\gamma_{42}x_4^{(2)} & \alpha_{34}-\gamma_{43}x_4^{(2)} & -m_4-\gamma_{43}x_3^{(2)} \end{bmatrix} = \begin{bmatrix} B & 0 \\ C & D \end{bmatrix}$$

Acknowledgments

I am grateful to Dr. Prof. Y.M. Svirezhev for the attention to the work and his kind criticism. He initiated the described method of the dynamical systems design based on storage-flow diagrams. I am also indebted to Dr. E.A. Denisenko for the useful discussion on the ecological meaning of mathematical results obtained in the model of carbon cycling in the mesotrophic bog ecosystem. This work was supported by the grant of the Russian Foundation for Basic Research #05-05-65137 and by the program "Hydrospheric and atmospheric processes: forming, changing and regulating the Earth Climate" of the Russian Academy of Sciences.

Appendix A

Proof of the Proposition 1.

$$\text{Jacobian matrix } J^{(1)} = \begin{bmatrix} -m_1-\alpha_{14} & -\gamma_{12}x_1^{(1)} & 0 & 0 \\ \gamma_{12}x_2^{(1)} & -m_2-\alpha_{24}+\gamma_{42}x_4^{(1)}+\gamma_{12}x_1^{(1)} & 0 & 0 \\ 0 & 0 & -m_3-\alpha_{34}+\gamma_{43}x_4^{(1)} & 0 \\ \alpha_{14} & \alpha_{24}-\gamma_{42}x_4^{(1)} & \alpha_{24}-\gamma_{43}x_4^{(1)} & -m_4 \end{bmatrix} = \begin{bmatrix} B & 0 \\ C & D \end{bmatrix},$$

is decomposable and hence its eigenvalues can be calculated from characteristic equations of two matrix blocks B and D:

(a) $\lambda_1^{(1)} = -m_1-\alpha_{14} < 0$; $\lambda_2^{(1)} = -m_2-\alpha_{24}+\gamma_{12}\frac{q_1}{m_1+\alpha_{14}}+\gamma_{42}\left(\frac{q_4}{m_4}+\frac{q_1\alpha_{14}}{m_4(m_1+\alpha_{14})}\right)$;

(b) $\det(D-\lambda I) = (-m_3-\alpha_{34}+\gamma_{43}x_4^{(1)}-\lambda)(-m_4-\lambda) = 0$ yields

$$\lambda_3^{(1)} = -m_4 < 0; \qquad \lambda_4^{(1)} = -m_3-\alpha_{34}+\gamma_{43}\left(\frac{q_4}{m_4}+\frac{q_1\alpha_{14}}{m_4(m_1+\alpha_{14})}\right).$$

Only $\lambda_2^{(1)}$ and $\lambda_4^{(1)}$ depend on bifurcation parameters and give curves $TC_{1,1}$, $TC_{1,2}$ in (3.5)–(3.6). □

Appendix B

Proof of the Proposition 2. As in the previous case, Jacobi matrix (3.4)

$$\begin{bmatrix} 0 & 0 & 0 & 0 \\ 0 & 0 & 0 & 0 \\ 0 & 0 & -m_3-\alpha_{34}+\gamma_{43}x_4^{(2)} & \gamma_{43}x_3^{(2)} \\ \alpha_{14} & \alpha_{24}-\gamma_{42}x_4^{(2)} & \alpha_{34}-\gamma_{43}x_4^{(2)} & -m_4-\gamma_{43}x_3^{(2)} \end{bmatrix} = \begin{bmatrix} B & 0 \\ C & D \end{bmatrix}$$

is decomposable, but can have two complex conjucate eigenvalues:

(a) $\lambda_1^{(2)} = -m_1-\alpha_{14} < 0$; $\lambda_2^{(2)} = -m_2-\alpha_{24}+\gamma_{12}(q_1/(m_1+\alpha_{14}))+\gamma_{42}((m_3+\alpha_{34})/\gamma_{43})$. Transcritical curve TC_2 of the second equilibrium is determined by equality $\lambda_2^{(2)} = 0$:

$$q_1 = \left(m_2+\alpha_{24}-\gamma_{42}\frac{m_3+\alpha_{34}}{\gamma_{43}}\right)\frac{m_1+\alpha_{14}}{\gamma_{12}} = \text{const.} = 949.5\ \text{g/(m}^2\ \text{year)}; \tag{5.3}$$

(b) $\det(D-\lambda I) = -(-m_3-\alpha_{34}+\gamma_{43}x_4^{(2)}-\lambda)(-m_4-\gamma_{43}x_3^{(2)}-\lambda)-\gamma_{43}x_3^{(2)}(\alpha_{34}-\gamma_{43}x_4^{(2)}) = \lambda^2+\lambda(m_4+\gamma_{43}x_3^{(2)})+m_3\gamma_{43}x_3^{(2)} = 0$. In this case, another transcritical curve is found from $m_3\gamma_{43}x_3^{(2)} = 0$, coinciding with the line $TC_{1,1}$ which indicates merging with steady state 1.

$\lambda_{3,4}^{(2)} = 1/2(-m_4-\gamma_{43}x_3^{(2)} \pm \sqrt{(m_4+\gamma_{43}x_3^{(2)})^2-4m_3\gamma_{43}x_3^{(2)}})$. Real part of these roots is negative iff $\text{tr}D < 0$, and $\det D > 0$, whereas

a neutrality curve denotes $-\text{tr}D = 0$, yielding Hopf bifurcation curve H_2 (3.8). □

Appendix C

Proof of the Proposition 3. Jacobi matrix (3.4) of the equilibrium 3

$$J^{(3)} = \begin{bmatrix} -m_1-\alpha_{14}-\gamma_{12}x_2^{(3)} & -\gamma_{12}x_1^{(3)} & 0 & 0 \\ \gamma_{12}x_2^{(1)} & 0 & 0 & \gamma_{42}x_2^{(3)} \\ 0 & 0 & -m_3-\alpha_{34}+\gamma_{43}x_4^{(3)} & 0 \\ \alpha_{14} & \alpha_{24}-\gamma_{42}x_4^{(3)} & \alpha_{24}-\gamma_{43}x_4^{(3)} & -m_4-\gamma_{42}x_2^{(3)} \end{bmatrix} \tag{C.1}$$

is decomposable (reservoir 3 can be distinguished) and has a cubic characteristic equation:

$$\lambda^3+k_1\lambda^2+k_2\lambda+k_3 = 0, \tag{C.2}$$

where coefficients are expressed through the matrix elements denoted as

$$J^{(3)} = \begin{bmatrix} p & r & 0 & 0 \\ s & d & 0 & e \\ 0 & 0 & f & 0 \\ g & h & k & m \end{bmatrix} : k_1 = -(p+m);\ k_2 = -(eh+rs-pm);\ k_3 = -reg+peh+mrs.$$

Transcritical curve $TC_{1,2}$ and fold curve $TC_{3,1}$ are following from the standard condition $k_3 = -reg+peh+mrs = 0$ which is expressed through the equilibrium components:

$$\gamma_{42}^2 x_2^{(3)} x_4^{(3)}(m_1+\alpha_{14}) - \alpha_{24}\gamma_{42} x_2^{(3)}(m_1+\alpha_{14}) - \gamma_{42} x_2^{(3)} \gamma_{12} x_2^{(3)} \alpha_{24} + \gamma_{42}^2 x_2^{(3)} x_4^{(3)} \gamma_{12} x_2^{(3)} + \gamma_{12}^2 x_1^{(3)} \left(x_2^{(3)}\right)^2 \gamma_{42} + m_4 \gamma_{12}^2 x_1^{(3)} x_2^{(3)} + \alpha_{14}\gamma_{42}\gamma_{12} x_1^{(3)} x_2^{(3)} = 0.$$

This equality can be transformed in $\gamma_{12} x_1^{(3)}(\gamma_{12}(m_4+\gamma_{42}x_2^{(3)}) + \alpha_{14}\gamma_{42}) = \gamma_{42}(m_1+\alpha_{14}+\gamma_{12}x_2^{(3)})(\alpha_{24} - \gamma_{42}x_4^{(3)})$, which gives transcritical curve $TC_{1,2}$ and the fold curve (4.9).

Straight line $TC_{3,2}$ can be obtained from equality $\lambda_1^{(3)} = -m_3 - \alpha_{34} + \gamma_{43} x_4^{(3)} = 0$ corresponding to the Jacobian element $J^{(3)}(3,3)$ which after substituting equilibrium values of storages acquires the form:

$$\gamma_{43}\left(\frac{m_2+\alpha_{24}}{\gamma_{42}} - \frac{\gamma_{12}}{2a\gamma_{42}}(-b \pm \sqrt{b^2-4ac})\right) = m_3 + \alpha_{34}. \qquad \text{(C.3)}$$

Eq. (C.3) in turn can be transformed:

$$\gamma_{43}^2\alpha_{24}q_1\gamma_{12} - \gamma_{42}(m_3+\alpha_{34})\gamma_{12}\gamma_{43}q_1 - m_4\gamma_{12}(m_3+\alpha_{34})K_1 + \gamma_{43}^2\alpha_{24}\gamma_{12}q_4 + \gamma_{43}^2 m_2 q_4 \gamma_{12} - \gamma_{42}(m_3+\alpha_{34})\gamma_{12}\gamma_{43}q_4 + K_1(m_2\alpha_{14}\gamma_{43} + (m_3+\alpha_{34})m_1\gamma_{42} - \gamma_{43}\alpha_{24}m_1) = 0, \qquad \text{(C.4)}$$

where $K_1 = \gamma_{43}(m_2+\alpha_{24}) - \gamma_{42}(m_3+\alpha_{34})$. From formula (C.4) the expression (4.10) for the line $TC_{3,2}$ immediately follows. □

REFERENCES

Alexandrov, G.A., Bazilevich, N.I., Logofet, D.O., Tishkov, A.A., Shytikova, T.E., 1994. Conceptual and mathematical modelling of matter cycling in Tajozhny Log bog ecosystem. In: Patten, B.C., et al. (Eds.), Wetlands and Shallow Continental Water Bodies, vol. 2. SPB Academic Publishing, The Hague, The Netherlands, pp. 45–93.

Allessina, S., Bondavalli, C., 2004. WAND: an ecological network analysis user-friendly tool. Environ. Model. Software 19, 337–340.

Bazilevich, N.I., Tishkov, A.A., 1986. Conceptual balance model of chemical matters cycling in a mesotrophic bog ecosystem. In: Bazilevich, N.I., Tishkov, A.A. (Eds.), Structure and Functioning of Southern Taiga Ecosystems, Institute of Geography. USSR Academy of Sciences, Moscow (in Russian).

Borrett, S.R., Whipple, S.J., Patten, B.C., Christian, R.R., 2006. Indirect effects and distributed control in ecosystems: temporal variation od indirect effects in a seven-compartment model of nitrogen flow in the Neuse River Estuary, USA—time series analysis. Ecol. Model. 194, 178–188.

Christensen, V., Walters, C.J., 2004. EcoPath with EcoSim: methods, capabilities and limitations. Ecol. Model. 172, 109–140.

Climo, R.S., 1984. The limits to peat bog growth. Philip. Trans. R. Soc. Lond. 303B, 605–654.

Climo, R.S., 1992. Models of peat growth. Suo 43, 127–136.

Fath, B.D., Borrett, S.R., 2006. A Matlab® function for Network Environ Analysis. Environ. Model. Software 21, 375–405.

Fath, B.D., Patten, B.C., 1998. Network synergism: emergence of positive relations in ecological systems. Ecol. Model. 107, 127–143.

Fath, B.D., Patten, B.C., 1999. Quantifying resource homogenization using network flow analysis. Ecol. Model. 123, 193–205.

Gattie, D.K., Schramski, J.R., Borrett, S.R., Patten, B.C., Bata, S.A., Whipple, S.J., 2006. Indirect effects and distributed control in ecosystems: network environ analysis of a seven-compartment model of nitrogen flow in the Neuse River Estuary, USA—steady state analysis. Ecol. Model. 194, 162–177.

Higashi, M., Patten, B.C., 1986. Further aspects of the analysis of indirect effects in ecosystems. Ecol. Model. 31, 69–77.

Higashi, M., Patten, B.C., Burns, T.P., 1993. Network trophic dynamics: the modes of energy utilization in ecosystems. Ecol. Model. 66, 1–42.

Jorgensen, S.-E., Svirezhev, Y.M., 2004. Towards a Thermodynamic Theory for Ecological Systems. Elsevier, 386 pp.

Kazanci, C., 2007. EcoNet: a new software for ecological modeling, simulation and network analysis. Ecol. Model. 208, 3–8.

Kuznetsov, Y.A., 1998. CONTENT—integrated environment for analysis of dynamical systems. Tutorial. Ecole Normale Superieure de Lyon, Rapport de Recherche UPMA-98-224.

Kuznetsov, Y.A., 2004. Elements of Applied Bifurcation Theory. Springer-Verlag, New York, 631 pp.

Latham II, L.G., 2006. Network flow analysis algorithms. Ecol. Model. 192, 586–600.

Logofet, D.O., 1997. Svicobians of the compartment models and DaD-stability of the Svicobians: aggregating '0-dimensional' models of global biogeochemical cycles. Ecol. Model. 104, 39–49.

Logofet, D.O., Alexandrov, G.A., 1983–1984a. Modelling of matter cycle in a mesotrophic bog ecosystem. I. Linear analysis of carbon environs. Ecol. Model. 21, 247–258.

Logofet, D.O., Alexandrov, G.A., 1983–1984b. Modelling of matter cycle in a mesotrophic bog ecosystem. II. Dynamic model and ecological succession. Ecol. Model. 21, 259–276.

Marsili-Libelli, S., Checchi, N., 2005. Identification of dynamic models for horizontal subsurface constructed wetlands. Ecol. Model. 187, 201–218.

Nungesser, M.K., 2003. Modelling microtopography in boreal peatlands: hummocks and hollows. Ecol. Model. 165, 175–207.

Pahl-Wostl, C., 1995. The Dynamic Nature of Ecosystems: Chaos and Order Entwined. Wiley.

Patten, B.C., 1982. Environs: realistic elementary particles for ecology. Am. Nat. 119, 179–219.

Patten, B.C., 1985. Energy cycling in the ecosystem. Ecol. Model. 28, 1–71.

Patten, B.C., 1992. Energy, emergy and environs. Ecol. Model. 62, 29–69.

Razumovsky, S.M., 1981. Patterns of Dynamics for Biogeocenoses. Nauka, Novosibirsk (in Russian).

Savageau, M.A., 1970. Biochemical systems analysis. III. Dynamic solutions using a power-law approximation. J. Theor. Biol. 26, 215–226.

Svirezhev, Y.M., 1997. On some general properties of trophic networks. Ecol. Model. 99, 7–17.

Tishkov, A.A., 1986. Productivity of bog ecosystems at the experimental area Tayozhny Log (Valdai district, Novgorod Region). In: Bazilevich, N.I., Tishkov, A.A. (Eds.), Structure and Functioning of Southern Taiga Ecosystems. Institute of geography RAS, Moscow (In Russian).

Ulanowicz, R.E., 1986. Growth and Development: Ecosystems Phenomenology. Springer, NY.

Ulanowicz, R.E., Abarca-Arenas, L.G., 1997. An informational synthesis of ecosystem structure and function. Ecol. Model. 95, 1–10.

Voit, E.O., Sands, P.J., 1996. Modeling forest growth. II. Biomass partitioning in Scots pine. Ecol. Model. 86, 73–89.

Yu, Z., Campbell, I., Vitt, D., Apps, M., 2001a. Modelling a long-term peatland dynamics. I. Concepts, review, and proposed design. Ecol. Model. 145, 197–210.

Yu, Z., Campbell, I., Vitt, D., Apps, M., 2001b. Modelling a long-term peatland dynamics. II. Processes and rates as inferred from litter and peat-core data. Ecol. Model. 145, 159–173.

Yu, Z., Li, C., Trettin, C., Li, H., Sun, G., 2002. An integrated model of soil, hydrology, and vegetation for carbon dynamics in wetland ecosystems. Global Biogeochem. Cycles 16 (4),1061.

Zavalishin, N.N., Logofet, D.O., 1997. Modelling ecological systems by a given “storage-flow” diagram. Matematicheskoe Modelirovanie (Math. Model.) 9 (9), 3–17 (in Russian with English summary).

Zavalishin, N.N., Logofet, D.O., 2001. Dynamic compartment models of the carbon cycle in a transitional bog ecosystem. Matematicheskoe modelirovanie (Math. Model.) 13 (4), 3–18 (in Russian with English summary).